Article

Camelina sativa Oilseed Cake as a Potential Source of Biopolymer Films: A Chemometric Approach to Synthesis, Characterization, and Optimization

Danijela Šuput [1], Lato Pezo [2], Slađana Rakita [3], Nedeljka Spasevski [3], Ružica Tomičić [1], Nevena Hromiš [1] and Senka Popović [1,*]

1. Faculty of Technology Novi Sad, University of Novi Sad, Bulevar cara Lazara 1, 21000 Novi Sad, Serbia; danijela.pejic@uns.ac.rs (D.Š.); ruzica.tomicic@uns.ac.rs (R.T.); nevena.krkic@uns.ac.rs (N.H.)
2. Institute of General and Physical Chemistry, University of Belgrade, Studentski Trg 12, 11000 Belgrade, Serbia; latopezo@yahoo.co.uk
3. Institute of Food Technology, University of Novi Sad, Bulevar cara Lazara 1, 21000 Novi Sad, Serbia; sladjana.rakita@fins.uns.ac.rs (S.R.); nedeljka.spasevski@fins.uns.ac.rs (N.S.)
* Correspondence: madjarev@uns.ac.rs; Tel.: +381-214853698

Abstract: In this work, the possibility of obtaining biopolymer films from *Camelina sativa* oilseed cake (CSoC) at different parameters of the synthesis process was investigated. The pH (values 8, 10, and 12), the temperature (60, 80, and 100 °C), and the concentration of the cake in the film-forming suspension (3, 4, and 5%) were varied. The films obtained were characterized by studying the mechanical, barrier, physico-chemical, structural, and biological properties (antioxidant and antimicrobial). The results showed moderate mechanical properties, indicating the application of these biopolymer materials as coatings. Low values of water vapor permeability (5.1–12.26 g/m^{2}h) and very low transmission in the UV range (less than 2%) indicate good barrier properties. FTIR analysis confirmed the films' composite structures: peaks related to proteins, polysaccharides, lipids, and cellulose were detected. The biological activity of the obtained CSoC films was pronounced so that they could be used for active packaging. All films have high antioxidant activity, which is more pronounced in samples synthesized at pH 8. The films possess antibacterial properties against *S. aureus*, while some had an inhibitory effect on *S. typhimurium*. Standard score analysis showed that the film sample synthetized at pH = 10, temperature = 100 °C, and concentration = 5% had optimal investigated properties.

Keywords: *Camelina sativa*; oilseed cake; valorization; biopolymer films; properties; optimization

1. Introduction

The number of by-products generated in agriculture during the processing and production of food has increased dramatically due to the demand for high-quality products. They are mainly generated during the processing of coffee, tea, wine, beer, sugar cane, fruit, and vegetables in the form of grain husks, fruit and vegetable peelings, leaves, seeds, etc., which are disposed of before and after harvesting, as well as by the end consumer, who often considers them unnecessary [1]. In recent years, the valorization of agro-industrial waste has been intensively studied [2]. There are many sources of waste: food waste in general [3] but in particular by-products from fruit and vegetable processing [4], by-products from grain processing [5], by-products from seafood processing [6], waste from the fishing industry [7], by-products from the dairy industry [8], by-products from edible oil processing [9], etc. There are also numerous potential applications for valorized waste, which include the conversion of agricultural waste into a raw material for the synthesis of various bioproducts, including organic acids, xylitol, xylo-oligosaccharides, biofuels, and biopolymers, as well as a substrate for enzymatic production [10].

Oilseed cakes and meals are valuable by-products of oilseed oil extraction, generally accounting for about 50% of the original seeds' total weight. The global production of

oilseeds, which are generally intended for edible oil production, reached 659 million metric tons in 2023 [11]. Solvents, hot (100 °C) or cold (50–60 °C) pressing, or green technologies (pulsed electric field, high voltage electric discharges, pressurized liquid, and high hydrostatic pressure) are the methods used to complete the extraction process [12]. Oilseed cakes are useful substrates for the extraction of valuable compounds (proteins, fibers, antioxidants, etc.), for pharmacological purposes, for the cosmetic industry, for the production of biofuels, and for edible film synthesis [12], depending on the variety and quality of the oilseeds, the method used for the extraction of the oil, and the cake quality. Taking into account their composition (high content of proteins, oils, and polysaccharides), these abundant, biodegradable, and low-cost materials present a promising substrate for the eco-friendly production of biopolymer packaging materials [9]. These materials have the potential to be successfully used in the food packaging sector and to replace at least a portion of non-biodegradable materials currently used [13].

The Brassicaceae family's annual oil crop, *Camelina sativa*, can be grown in a variety of climates with low water and nutrient requirements [14,15]. It can be grown with little to no irrigation, little fertilizer, and often on marginal or saline soils [16]. Due to its strong resistance to microbiological diseases and insect pests, its cultivation is less harmful to the environment as fewer pesticides and herbicides are needed [17,18].

Camelina seeds are garnering renewed attention due to their rich nutritional profile. Camelina stands out as a leading candidate for use in the bioeconomy thanks to its intriguing fatty acid profiles among oilseeds [19]. Oil (30% to 49%), protein (24% to 31%), carbohydrates, dietary fibers, ω-3 and ω-6 acids, tocopherols, phytosterols, and phenolic compounds, among other nutrients, are abundant in camelina seeds [20–22]. Furthermore, camelina seeds have an underestimated concentration of mucilage, a soluble fiber found in the seed's outermost layer, known as the mucilaginous epidermis. In addition to the bioactive compounds of mucilage, which play an important role in its health-promoting properties [23], the mucilage of camelina seeds may be a new source of hydrocolloids with thickening, gelling, emulsifying, and stabilizing properties. Therefore, it has the potential to be used in a variety of pharmaceutical and food applications [23,24]. Recently, camelina oilseed oil has been granted Generally Recognized as Safe (GRAS) status by the USFDA [24]. Each year, there has been a notable increase in the amount of camelina-related literature; this growth became particularly evident in patent documents after 2009 and in scholarly publications after 2010 [25].

Oilseed cake (pomace), the principal by-product of camelina seeds, is currently used as a raw material in a variety of applications. Camelina cake is a product of oil extraction obtained by pressing camelina seeds. Currently, biofuel (biodiesel, jet fuel), functional food, diet supplements, bio-lubricants, chemical derivatives, animal feed, and soil fertilizer products, including ethanol, biogas, energy pellets, and compost, are made from seeds and straw. The current uses of camelina emerged from an analysis of over a thousand sources of scientific literature [25]. Various fractions of *Camelina sativa* have been utilized to produce new materials or to improve the properties of existing materials. Most of the works used camelina oil, while other research has considered camelina proteins [26]. To the authors' knowledge, no research has yet been conducted on obtaining biopolymer materials from whole camelina oilseed cake.

In our previous study [27], the effect of cake granulation and the presence of mucilage on film properties was investigated, and it was concluded that biopolymer films based on camelina with the lowest cake granulation and with the presence of naturally occurring mucilage exhibited optimal film properties. In this regard, the aim of the present study was to synthesize, characterize, and optimize the development of biopolymer film based on camelina cake with particle sizes of less than 180 nm and the presence of naturally occurring mucilage, considering synthesis process parameters—pH and temperature—and the initial concentration of the camelina cake (the input parameters). By studying the output parameters and physico-chemical, mechanical, barrier, and structural characteristics of the obtained films and by applying appropriate mathematical models, optimal process

parameters will be selected. The synthesis routes of biopolymer films based on different oilseed cakes have been presented in the literature so far. The novelty of this work is the synthesis and optimization of biopolymer material based on *Camelina sativa* cake, which has not been examined for this purpose till now. The purpose of this work was to optimize the properties of the obtained films depending on the applied process parameters, while the ultimate aim is the application of the obtained material for the packaging of the selected food product.

2. Materials and Methods

2.1. Materials

Camelina sativa seeds were kindly supplied by the Institute of Field and Vegetable Crops (Novi Sad, Serbia). To extract oil, camelina seeds were mechanically cold-pressed. The resulting cake was crushed and sieved by use of a universal laboratory sifter (Bühler AG, Uzwil, Switzerland) equipped with a stack of sieves (fraction < 180 μm). The fraction of cold-pressed camelina seed cake < 180 μm (CSoC) was used for biopolymer film preparation. CSoC fraction exhibited a chemical composition comprising 39.4% protein, 19.4% oil, and 5.9% cellulose. CSoC was kept in storage at 4 °C before analysis. All other reagents used in this study were of analytical grade.

2.2. Experimental Design

The influence of the process parameters (pH (X_1): 8–10–12; temperature (X_2): 60 °C–80 °C–100 °C; and concentration (X_3): 3%–4%–5%) on film physico-chemical, mechanical, barrier, structural, and antioxidant properties was investigated using a three-level, three-factor Box–Behnken response surface design (BBD) with three central point replicates. Fifteen experimental runs are presented in Table 1. A second-order polynomial model was used to fit the experimental data:

$$Y = \beta_0 + \Sigma\beta_i X_i + \Sigma\beta_{ij} X_i X_j + \Sigma\beta_{ii} X_i^2 + e_i$$

where various X_i values are independent variables affecting the responses Y. β_0, β_i, β_{ii}, and β_{ij} are the regression coefficients for intercept and interaction coefficients of linear, quadratic, and second-order terms, respectively, while k is the number of variables [28].

Table 1. Box–Behnken experimental design with process variables (uncoded) and obtained responses.

RUN	pH	t°	c	MC	S	t	TS	EB	WVP	AO
1	8	60	4	25.93 ± 1.27 def	33.02 ± 0.15 de	228.33 ± 1.53 c	0.54 ± 0.01 ab	16.66 ± 1.5 f	9.40 ± 0.09 e	76.86 ± 5.21 e
2	12	60	4	31.70 ± 0.09 gh	40.92 ± 0.57 f	221.33 ± 4.04 bc	0.59 ± 0.02 bc	5.75 ± 0.75 ab	7.92 ± 0.03 cd	29.13 ± 1.53 b
3	8	100	4	24.69 ± 1.14 cde	25.91 ± 2.85 bc	238.67 ± 3.79 d	0.96 ± 0.03 ef	7.40 ± 2.15 abc	8.21 ± 0.07 cde	77.32 ± 3.45 e
4	12	100	4	23.69 ± 2.03 cd	44.57 ± 3.21 f	246.67 ± 3.05 de	1.85 ± 0.07 j	9.85 ± 1.06 cde	6.46 ± 0.05 b	23.47 ± 1.89 ab
5	8	80	3	29.12 ± 1.08 fg	26.02 ± 1.67 bc	245.33 ± 2.89 de	0.93 ± 0.02 e	9.69 ± 0.68 cde	6.21 ± 0.05 ab	70.55 ± 4.28 de
6	12	80	3	28.25 ± 2.25 efg	42.53 ± 0.32 f	215.33 ± 3.51 ab	0.53 ± 0.01 ab	10.54 ± 1.31 cde	7.84 ± 0.11 cd	16.44 ± 1.02 a
7	8	80	5	27.60 ± 1.30 defg	29.48 ± 1.11 cde	292.33 ± 3.51 g	0.70 ± 0.01 d	12.52 ± 0.57 de	6.45 ± 0.38 b	75.35 ± 3.62 e
8	12	80	5	21.44 ± 2.00 bc	41.42 ± 1.11 f	294.67 ± 3.51 gh	1.24 ± 0.02 h	12.88 ± 0.63 e	6.94 ± 0.06 bc	23.60 ± 0.89 ab
9	10	60	3	37.21 ± 1.53 i	20.58 ± 0.45 a	209.67 ± 2.52 a	0.62 ± 0.01 c	5.77 ± 0.80 ab	12.26 ± 0.82 f	69.56 ± 2.12 de
10	10	100	3	34.28 ± 0.80 hi	21.85 ± 1.52 ab	270.33 ± 3.21 f	1.76 ± 0.03 i	4.34 ± 0.15 a	5.10 ± 0.53 a	69.25 ± 2.08 de
11	10	60	5	17.35 ± 1.38 ab	32.83 ± 1.78 de	302.33 ± 4.51 h	0.49 ± 0.02 a	10.60 ± 0.98 cde	8.02 ± 0.73 cd	69.89 ± 3.05 de
12	10	100	5	13.86 ± 1.53 a	34.52 ± 3.05 e	292.67 ± 2.52 gh	1.03 ± 0.01 fg	8.83 ± 0.56 cb	5.86 ± 0.30 ab	66.01 ± 3.56 d
13	10	80	4	28.69 ± 0.98 efg	24.82 ± 1.77 abc	244.33 ± 4.51 de	1.07 ± 0.02 g	8.76 ± 1.16 cb	9.10 ± 0.78 de	78.04 ± 1.69 e
14	10	80	4	14.60 ± 0.73 a	26.62 ± 0.74 bc	245.67 ± 2.52 de	0.94 ± 0.02 ef	10.30 ± 1.87 cde	9.03 ± 0.65 de	52.47 ± 1.98 c
15	10	80	4	28.17 ± 0.39 efg	28.10 ± 1.91 cd	251.00 ± 2.00 d	0.97 ± 0.01 ef	9.32 ± 0.66 cd	8.96 ± 0.42 de	55.16 ± 3.11 c

a–i Means in the same column with different superscripts are statistically different ($p \leq 0.05$). MC (%)—moisture content; S (%)—solubility; t (μm)—thickness; TS (MPa)—tensile strength; EB (%)—elongation at break; WVP (g/m^{2}h)—water vapor permeability; AO (%)—antioxidative potential (DPPH).

2.3. Biopolymer Film Preparation

Biopolymer films based on *Camelina sativa* oilseed cake (CSoC) were prepared using the casting method. The filmogenic suspension was prepared by dispersing CSoC (different concentrations: 3%–5%, *w/v*) in distilled water with 40% glycerol (*w/w*, by weight of CSoC) as a plasticizer. The pH of all samples was further adjusted to different pH (8–12) values by

adding NaOH solution, which was determined using a pH meter (Metrohm AG, Herisau, Switzerland). In the next step, the resulting suspension was incubated in a water bath at different temperatures (60–100 °C) for 20 min. After heat treatment, the suspension was passed through a nylon filter to remove the cake's coarse, undissolved particles. A total of 50 g of film-forming suspension was poured onto Petri plates, covered with Teflon, and allowed to dry for five days at room temperature (23 ± 2 °C, 50 ± 5% RH). The produced films were removed from Petri plates and analyzed after drying.

2.4. Biopolymer Film Characterization

2.4.1. Film Thickness

Film thickness was conducted with 1 μm sensitivity micrometer DIGICO (TESSA, Poschiavo, Switzerland). Film thickness was expressed as mean values of eight repetitions ± SD.

2.4.2. Mechanical Properties

Tensile strength (TS) and elongation at break (EB) were measured in accordance with the standard method EN ISO 527-3:2018 [29] by using the Instron Universal Testing Instrument 4301 (Instron Engineering Corp., Canton, MA, USA). The initial distance between the instrument clamps was 50 mm, while the speed was 50 mm/min. Eight replicates were carried out on each sample. The result was expressed as mean ± SD.

2.5. Barrier Properties

2.5.1. Water Vapor Permeability

The water vapor permeability (WVP) of the obtained films was determined according to standard method ISO 2528:2017 [30]. The rate of water vapor transfer through the sample was determined by calculating the difference in the mass of the silica gel before and after treatment (indicating absorbed moisture), dividing it by the surface area of the film sample, and expressing the result in grams per square meter per hour (g/m^2h). Three tests were performed for each sample, and the result was expressed as mean ± SD.

2.5.2. Light Transmission

The ultraviolet (UV) and visible light transmittance properties of the films were measured at wavelength range from 200 nm to 800 nm (with 5 nm step) using a UV spectrophotometer (T80/T80+ UV-VIS Spectrophotometer PG Instruments Ltd., Lutterworth, UK). Three tests were performed for each sample, and the result was expressed as mean ± SD.

2.6. Physico-Chemical Properties

Moisture Content

Film samples (1×1 cm^2) were weighed at analytical balance (m_1) and dried in an air-circulating oven at 105 ± 2 °C (Instrumentaria, Zagreb, Croatia) until constant weight (m_2). The moisture content (MC) was determined as the percentage of weight reduction after film drying, expressed on the total weight of the film:

$$MC\ (\%) = ((m_1 - m_2)/m_1) * 100$$

The result was expressed as the mean value of three independent measurements ± SD for each sample.

2.7. Film Solubility

Immediately after determining the moisture content, the film samples (1×1 cm^2), dried to constant mass, were used to determine the film solubility. Each film sample was weighed (m_1), immersed in 30 mL of deionized water, and allowed to stand for 24 h at room conditions, with occasional shaking. After 24 h, the water was decanted, and the films were dried again in an oven (Instrumentaria, Zagreb, Croatia) at (105 ± 2) °C to a

constant mass (m_2). The total solubility of the films (%) was calculated according to the following equation:

$$S\ (\%) = (m_1 - m_2)/m_1 * 100$$

where m_1 represents the dry matter of the film before dissolving in water, and m_2 is the dry matter of the film after dissolution in water and drying. The test for determining the total solubility was performed in three independent replicates, and the results are provided as mean $\pm$ SD.

2.8. Film Morphology

The surface morphology of the obtained film samples was analyzed by using scanning electron microscopy (SEM Hitachi TM3030, Hitachi High Technologies, Tokyo, Japan) under a high vacuum (acceleration voltage 15 kV, beam current 20 nA).

2.9. Structural Properties—Fourier-Transform Infrared Spectroscopy (FTIR)

Structural properties were determined according to method ASTM D5576:00 (2021) [31] by using Nicolet IS10 FT-IR spectrophotometer (Thermo Fisher Scientific, Waltham, MA, USA) and attenuation total reflection (ATR) extension. All spectra were recorded in the spectral range 4000–400 cm^{-1} at a resolution of 4 cm^{-1}. Each sample was scanned 16 times, while a blind sample (background) was recorded before analyzing each sample. Software Omnic 8.1. (Thermo Fisher Scientific, Waltham, MA, USA) was used to collect, manage, and process the FTIR spectra.

2.10. Antioxidative Activity
2,2-Diphenyl-1-picrylhydrazyl (DPPH) Assay

A piece of film (1×1 cm^2) was placed in a bottle containing 2 mL of a freshly prepared DPPH$^{\bullet}$ solution (0.0185 g DPPH$^{\bullet}$ in 50 mL ethanol) diluted in ethanol (1:5), and the mixture was stirred for 24 h in a dark chamber at room temperature. In each sample, the residual DPPH$^{\bullet}$ concentrations were determined after the removal of the solid film and by measuring the absorbance at 520 nm using a T80/T80+ UV-VIS spectrophotometer (PG Instruments Ltd., Lutterworth, UK). The control sample (blank) is the sample in which there was no film. The antioxidant activity of the films was expressed as a percentage and calculated according to the following formula:

$$AO\ (\%) = ((DPPH^{\bullet}_0 - DPPH^{\bullet}_s))/(DPPH^{\bullet}_0) * 100$$

where DPPH$^{\bullet}_s$ is the concentration of DPPH$^{\bullet}$ in the tested film sample, and DPPH$^{\bullet}_0$ is the concentration of DPPH$^{\bullet}$ in the corresponding blank. For each film, the test was repeated three times, and the result was presented as mean $\pm$ SD.

2.11. Antimicrobial Activity
Disc Diffusion Method

Two Gram-negative bacteria, *Escherichia coli* ATCC 10536 and *Salmonella typhimurium* ATCC 14028, and two Gram-positive bacteria, *Staphylococcus aureus* ATCC 25923 and Listeria monocytogenes ATCC 19111, were used to study the antibacterial activity of CSoC film samples. They were selected because of their importance in the food industry as the most common pathogenic and spoilage bacteria. The reference strains were purchased lyophilized from the American Type Culture Collection (Manassas, VA, USA) and stored in the culture collections of the Institute of Food Technology, University of Novi Sad. All strains were stored at $-80\ ^{\circ}$C in Trypto-casein Soy Broth (TSB; Biokar BK046 HA, Beauvais, France) supplemented with 15% glycerol. Prior to the experiments, the strains were revitalized by cultivation on tryptic soy agar (TSA; Oxoid CM0131, Hampshire, UK) for 24 h at 37 $^{\circ}$C. A loop of actively growing cells of each strain was suspended in phosphate-buffered saline (PBS; Oxoid, Hampshire, UK, pH 7.3) and adjusted to match the turbidity

of a 0.5 McFarland standard. For the antimicrobial activity assays, bacterial suspension was diluted in TSB to achieve a final cell concentration of 1×10^6 CFU/mL.

The disc diffusion method was used to study the antibacterial activity of fifteen CSoC films, as previously reported [32], with some modifications. The tests were also conducted using ampicillin (Bioanalyse, Ankara, Turkey) for bacteria as a control for microorganism sensitivity. In brief, TSA agar plates were inoculated with 100 μL/mL of each cell suspension (1×10^6 CFU/mL) prepared as above, and sterile filter paper discs (6 mm diameter) were placed on the agar surface. The discs were then inoculated with 10 μL of a stock solution of each CSoC film, and then plates were incubated at 37 °C for 24 h. Antibacterial activity was evaluated by measuring the diameter of the inhibition zone around the discs and was expressed as the mean zone of inhibition diameters (mm) produced by *Camelina sativa*. The assay was performed in three replicates for each strain.

2.12. Statistical Analysis
Principal Component Analysis

Principal component analysis (PCA) was utilized to uncover connections between variables showing analogous interactions. The impact of process parameters—pH (ranging from 8 to 12), temperature (ranging from 60 °C to 100 °C), and concentration (varying from 3% to 5%)—on the physical, chemical, mechanical, barrier, structural, and antioxidative attributes of the film was investigated. This exploration employed a Box–Behnken response surface design (BBD) consisting of three factors at three levels each, including three central point replicates. The findings from 15 experimental runs are detailed in Table 1.

2.13. Correlation Analysis

The color-coded diagram was created using R software version 4.0.3 (64-bit version) to visualize the mean values of all observed responses. The "corrplot" function was used with the "circle" method and upper type activated to visualize the correlations between the different responses observed in the samples.

2.14. Standard Score

Standard scores were assessed across various process parameters, and application trials were conducted using the casting process. The ranking system hinged on the comparison between the original data and the highest and lowest values observed for each output variable [33]. As optimal output variable values, the lowest values of MC, S, and WVP and the highest values of TS, EB, and AO were set.

2.15. Artificial Neural Network Modeling

In the subsequent stage of the research, a mathematical model, specifically an artificial neural network, was developed. This model's objective was to forecast physical, chemical, mechanical, barrier, structural, and antioxidative properties of the film. It operated based on inputting process parameters encompassing pH values (ranging from 8 to 12), temperatures (ranging between 60 °C and 100 °C), and concentrations (ranging from 3% to 5%).

Initially, the dataset underwent division, allocating 70% for training the model and reserving 30% for testing. This division method adhered to a standard approach as detailed in the investigation by [34]. Following data preparation, regression models were constructed based on Equation (1) as outlined by [35]:

$$Y = f_1(W_2 \cdot f_2(W_1 \cdot X + B_1) + B_2) \tag{1}$$

Y—output value; f_1, f_2—transfer functions of the hidden and output layers; $W_{1,2}$—weight coefficients of the hidden and output layers; $B_{1,2}$—hidden and output layer biases.

Upon computing the output values, a series of statistical error tests and residual analyses were conducted. These encompassed the chi-square test (χ^2), root mean square

error (*RMSE*), mean bias error (*MBE*), mean percentage error (*MPE*), sum squared error (*SSE*), and average absolute relative error (*AARD*) [36,37]:

$$x^2 = \frac{\sum_{i=1}^{N} (x_{p,i} - x_{e,i})^2}{N - n} \tag{2}$$

$$RMSE = \left[\frac{1}{N} \cdot \sum_{i=1}^{N} (x_{p,i} - x_{e,i})^2 \right]^{1/2} \tag{3}$$

$$MBE = \frac{1}{N} \cdot \sum_{i=1}^{N} (x_{p,i} - x_{e,i}) \tag{4}$$

$$MPE = \frac{100}{N} \cdot \sum_{i=1}^{N} \left(\frac{|x_{p,i} - x_{e,i}|}{x_{e,i}} \right) \tag{5}$$

$$SSE = \sum_{i=1}^{N} (x_{p,i} - x_{e,i})^2 \tag{6}$$

$$AARD = \frac{1}{N} \cdot \sum_{i=1}^{N} \left| \frac{x_{e,i} - x_{p,i}}{x_{e,i}} \right| \tag{7}$$

where p in the index and exponent stands for predicted values, and e in the index and exponent stands for experimentally determined values.

2.16. Data Manipulation

The statistical analysis involved calculating the mean and standard deviation of categorized data. To assess differences among the observed categories, analysis of variance was employed. The data were processed using the TIBCO STATISTICA software package ver. 12 (2021), which was tailored to suit the specific dataset.

3. Results

3.1. Visual Appearance

The obtained CSoC films were opaque and dark in color, ranging from brownish-yellow to brown (Figure 1). It was noticed that these colorations were more intense for films prepared at higher pH values. The smell of all films is neutral to slightly pronounced, similar to the smell of the camelina oilseed cake. All films have good tactile characteristics—they are thin, firm, and flexible.
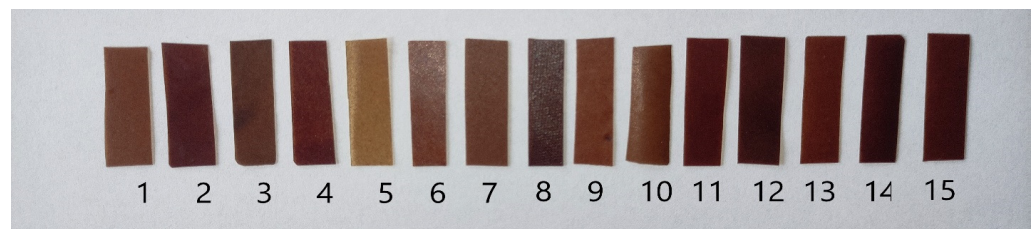

Figure 1. Visual appearance of *Camelina Sativa*-based biopolymer films (labels (runs) 1–15 refer to different processing conditions (see Table 1)).

3.2. Mechanical Properties

When employed as both a package and as an integral edible layer around the food product, the film or coating should offer a continuous overall structure during the storage time. Therefore, the mechanical qualities are crucial for the application and even consumption [38]. The obtained TS values are in the range of 0.49–1.89 MPa, while EB values were in the range of 4.34%–16.66% (Table 1). These low values are common for

biopolymer films based on oilseed cakes. The highest TS value was measured for the sample prepared at pH 12, 100 °C, and a concentration of 4%, while the highest EB value was measured for the sample prepared at pH 8, 60 °C, and a concentration of 4%. The obtained low TS and EB values do not necessarily eliminate biopolymer films in packaging applications. These mechanical properties of the material point to application in the form of coatings.

Based on data in the literature, the TS values of biopolymer films based on chitosan ranged up to 40 MPa [39], and for biopolymer films based on cellulose derivatives, TS values ranged up to 60 MPa [40], while the TS values of alginate-based films were around 70 MPa [41]. On the other hand, TS values for protein-based biopolymer films had a range of 2.3 MPa for sunflower protein-based films [42], 6 MPa for fish-based protein-based films [43], 11 MPa for films based on soy protein isolate [44], 1.37 MPa for biopolymer films based on pumpkin oil cake [45], 4.37 MPa for biopolymer films based on sunflower oil cake [46], 1.7 MPa for cardoon oilseed cake protein-based films [47], and 1.4–3.65 MPa for films based on rapeseed oil cake [48]. In the research of Petraru and Amariei [49], the addition of sunflower oil cake to sodium alginate films led to a decrease in TS from 27.11 MPa to 8.66 MPa. This mechanism, in which the tensile strength decreases with increasing the hydrophobic lipid component, was attributed to the weakening of the protein structure, and that resulted in decreased TS of the films [38].

The EB values in this paper ranged from 4.34% to 16.66%. The literature shows that the EB values range from 5% for films based on pumpkin oilseed cake [50] to 11.62%–20.62% for films based on rapeseed oil cake [48], 20%–30% for films based on sunflower oilseed cake [42,46], 69.54%–77.92% for films based on soy protein isolate and sunflower oil [38], around 140% for cardoon oilseed cake protein-based films [47], and 148% for fish protein-based films [43]. The EB is lower than in other research, which could be attributed to various aspects of the film production process. Proteins make up the largest proportion of the composition of the cake, so the cross-linking between them has the greatest influence on the low EB. Under the extreme conditions of film formation (high t and high pH), the strongest protein denaturation takes place, during which the intermolecular bonds are loosened. During film formation, the released bonds can react and form a dense protein network, resulting in rigid films with low EB. High processing temperatures cause a more intense denaturation of the proteins, independent of the applied pH values, resulting in low EB values. At lower processing temperatures, denaturation is not complete at low pH, while higher pH values intensify denaturation, which determines the differences in EB values.

3.3. Barrier Properties

3.3.1. Water Vapor Permeability

The WVP of films is an important property that strongly influences the usefulness of films in food packaging systems. This property is also a known drawback of most hydrocolloid films, limiting their applicability in food packaging. WVP is influenced by thickness, composition, linkage, and hydrophilicity [49]. The values obtained for CsoC film were in the range of 5.1–12.26 g/m^2h (Table 1) and consistent with findings in the literature for sunflower oil cake-based films (8.62 g/m^2h to 11.63 g/m^2h [46], pumpkin oil cake-based materials (14.7 g/m^2h) [51], and argan seed protein concentrate (7.5 g/m^2h) [13].

According to Abdollahi et al. [52], the ratio of hydrophilic to hydrophobic components in the film determines how the water vapor is transferred, with the hydrophilic part of the film serving as the primary conduit. For this reason, adding more hydrophobic components to the film matrix can lead to a reduction in the water vapor permeability of biopolymer materials. The lower WVP values obtained in this research are a result of naturally occurring lipid components in oil cakes. Regarding the process parameters, the samples with higher oil cake concentration (5% and 4%)—samples 4, 7, 8, and 12—were found to have lower WVP values. The higher oil cake concentration increases the viscosity of the film-forming suspension and makes the films thicker and denser, resulting in lower WVP [49,53].

3.3.2. Light Transmission

Photolysis and photo-oxidation reactions in connection with prolonged exposure to light, particularly UV light, have an impact on the quality of food. The production of free radicals and active oxygen, the development of disagreeable odors, and a decrease in food's nutritional content cause food to deteriorate [54]. Consequently, one of the key factors in extending the shelf-life of packaged food is the packing material's ability to prevent photo-oxidation through UV-blocking qualities [47]. In terms of UV-VIS spectral qualities, the lowest possible transmittance of UV radiation (which prolongs the shelf life of packaged foods) and higher possible transparency in the visible range (which provides consumers visual control) are necessary [12].

The spectra of all tested CsoC film samples, presented in Figure 2, exhibited a similar pattern: very low transmission in the UV range (less than 2%), which increases after 400 nm but does not exceed 6.2% (for sample 2). All films block the transmission of light below 400 nm almost completely and, therefore, offer excellent UV protection over the entire UV wavelength range. It is assumed that the low light transmittance of composite films is most likely the cause of their chemical composition, i.e., a large number of polyphenolic compounds, aromatic amino acids, cellulose, and lignin, which have potential UV-blocking properties [47,55]. In the visible range (400–800 nm), all films showed low transmission values and thus offered low visual access due to the dark color of the films so that the opaque films could be used as food preservatives against light transmission. Therefore, edible films based on CsoC can be used for packaging foods that are susceptible to oxidative changes catalyzed by UV light. Similar conclusions were made by Fang et al. [56] after the analysis of edible films obtained from whey proteins, as well as by Priyadarshi et al. [57] after the analysis of pectin–pullulan-based films with grape seed extract addition.
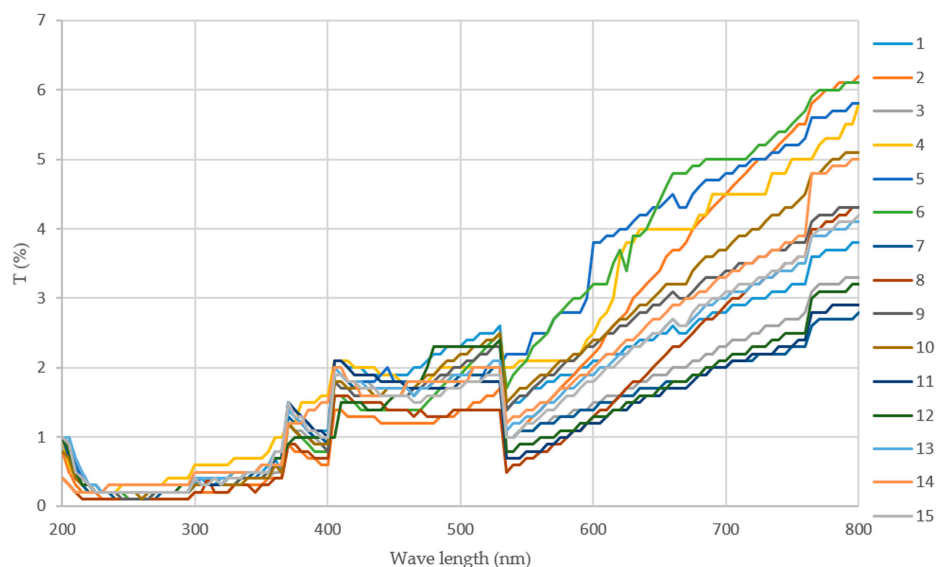

Figure 2. Light transmission of *Camelina Sativa*-based biopolymer films (labels (runs) 1–15 refer to different processing conditions (see Table 1)).

3.4. Physico-Chemical Properties

3.4.1. Moisture Content

Moisture content is an important biopolymer film characteristic because it affects other film properties. The moisture content values ranged from 13.86% to 37.21% (Table 1). From the observed range of moisture content values and applied synthesis process parameters, it can be concluded that films with a higher initial concentration of camelina cake have lower moisture content values. This may be due to the higher content of cake components (proteins, carbohydrates, fibers).

The obtained values were slightly higher than the moisture content of other films based on oil cakes found in the literature. The moisture content of composite films based on soy protein isolate and sunflower oil was 33.25% [38], while the moisture content of composite films based on whole sunflower oil cake was 13.76%–20.47% [46]. The moisture content of films obtained from sunflower protein concentrates was 34.1% [58], that of pumpkin oil cake-based films was 19.78% [45], and that of cardoon protein-based films was around 17% [47].

3.4.2. Film Solubility

Films' water solubility indicates their integrity in an aqueous environment; higher WS signifies lower water resistance. The structural characteristics of proteins and the presence of other non-proteinaceous components in the films, primarily phenolic compounds, carbohydrates, and minerals, are directly related to the water solubility of the obtained films and may influence its hygroscopicity as well as other factors like the film's thickness and water content [58].

The solubility obtained for the films was relatively low (20.58%–44.57%) (Table 1) compared with the data in the literature. The water solubility of the hemp protein film was 41%, that of the cardoon protein film was 52%, that of the argan protein film was 43% [13], and that of soy protein isolate and sunflower oil was 50.01% [38], while the water solubility of films obtained from sunflower protein concentrate was 96.9% [58]. It is noteworthy that, even after immersing in water for 24 h, all the films maintained their structural integrity. Lower concentrations of camelina oil cake and medium pH contributed to the lower values of the water solubility.

3.5. Film Morphology

The results obtained using SEM microscopy showed that CSoC-based films have a compact surface (Figure 3), pointing to dense morphology, which is typical for protein-based films [59,60]. No cracks or ruptures were observed on the surface, which, along with the compact structure, affects the film's good barrier properties. The quantity and size of voids have an impact on the films' barrier qualities. This is in agreement with Petraru and Amarei findings [49], who examined the microstructure of sunflower oil cake-based films, and Luo et al. [61], who examined sodium alginate-based green packaging films functionalized by guava leaf extracts.
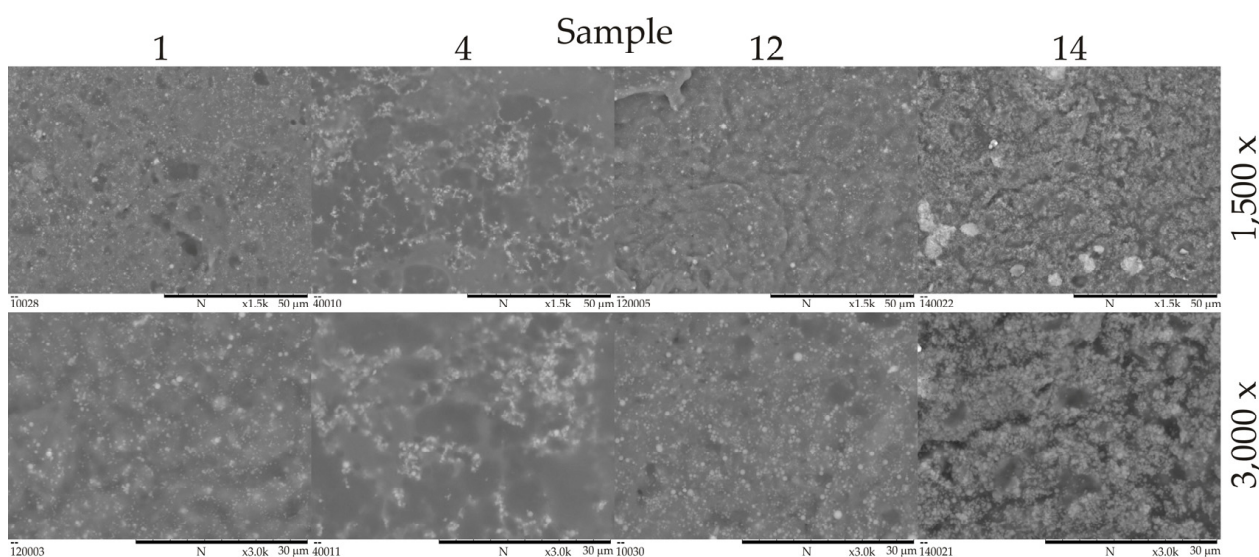

Figure 3. Surface morphology of *Camelina Sativa*-based biopolymer films (labels (runs) 1, 4, 12, and 14 refer to different processing conditions (see Table 1)).

SEM images show an uneven surface with a rough structure. According to Erdem and Kaya [38], an explanation for an uneven film surface with a discontinuous and rougher structure was associated with reduced lipid miscibility in the matrix. Because the oil droplets were not well-retained by the film matrix, they were able to appear on the surface of the film. This was also reported by Mirpoor et al. [13], who prepared argan oilseed cake-based films, and Delgado et al. [62], who prepared films derived from rapeseed protein concentrate. The same effect on the film morphology had the addition of sunflower oil cake to the sodium alginate films since they showed rougher but still continuous structures. The roughness increased with the increasing amount of SFOC added due to the increase in fibrous particles [49].

Some scattered microcrystals, the most noticeable in CSoC-based film sample 14, are present in the microstructure. They might be a consequence of the use of sodium hydroxide during the protein extraction process. In the investigation of protein extracted from castor bean cake [60], the components present in the microcrystals were additionally determined by the elemental analyzer coupled to SEM and identified as potassium (2.6%), sodium (2.4%), and sulfur (1.8%).

3.6. Structural Properties—Fourier-Transform Infrared Spectroscopy (FTIR)

The obtained CSoC-based films were subjected to FTIR spectral analysis to evaluate the possible effects of the process parameters on the structural properties. After FTIR analysis, all spectra showed peaks at the same wavelengths with different intensities, indicating that the applied process parameters affected the structural properties of the obtained CSoC films (Figure 4a). However, the spectra obtained were heterogeneous, so it was not possible to highlight one of the process parameters and conclude that it influenced the structure of the film to a significant extent. If, for example, the temperature was to be singled out, not all samples synthesized at the highest temperature showed maximum absorbances for specific wavelengths.

The broad band at 3500–3000 cm^{-1} (centered at around 3260–3280 cm^{-1}) corresponds to the O–H stretching and C–H stretching vibration. Similar results were reported in the studies of chia seed mucilage/chitosan composite films [63], edible films from pea starch and casein [64], active packaging material based on starch [65], and nanocomposite polymer films based on levan and chia seed mucilage [66]. The maximum absorbance at this wavelength was recorded for sample 6 (pH 12, T 80 °C, conc. 3, A = 0.143), and the minimum was for sample 11 (pH 10, T 60 °C, conc. 5, A = 0.096). The asymmetric stretching of CH_2 and CH is the cause of the appearance of the peak at 2925 cm^{-1}, which might originate from present proteins or cellulose molecules, which was also confirmed in [67,68]. The peak at around 1740 cm^{-1} (from the C=O stretching vibration of triglycerides) is associated with the carbonyl ester group in lipid molecules [69], and it is related to the lipid content [70]. The maximum absorbance value for this peak was observed in sample 11 (pH 10, T 60 °C, conc. 5, A = 0.0340), and the minimum was for sample 6 (pH 12, T 80 °C, conc. 3, A = 0.0167).

Fourier-transform infrared spectra of the CSoC-based films produced with proteins extracted at different pH revealed Amide I (between 1600 and 1700 cm^{-1}) and Amide II (1470–1570 cm^{-1}) bands [71], representing different vibrational modes associated with the peptide bonds, which is in agreement with [60]. In addition to the C=O stretching vibration, the C–N bond stretching vibration also contributes to Amide I, which is the most significant peak for FTIR analysis of secondary protein structures. The large peak in the Amide I region at 1653–1655 cm^{-1} was ascribed to α-helix, and it correlates with Wachirattanapongmetee et al.'s [70] findings, which differentiate protein types extracted from tilapia by-products. Amide II is generated by N–H bending vibration and C–N stretching vibration [72]. According to [70], α-helical structure is denoted by a peak in the Amide II region at 1544 cm^{-1}. In the case of CSoC-based films, this peak was shifted to 1539 cm^{-1}. When a molecule's peak shifts to the lower wave number side, its mass increases because the mass of a vibrating molecule is inversely related to its frequency of

oscillation. Therefore, lower wave numbers and lower vibration frequencies correspond to heavier molecules [73].
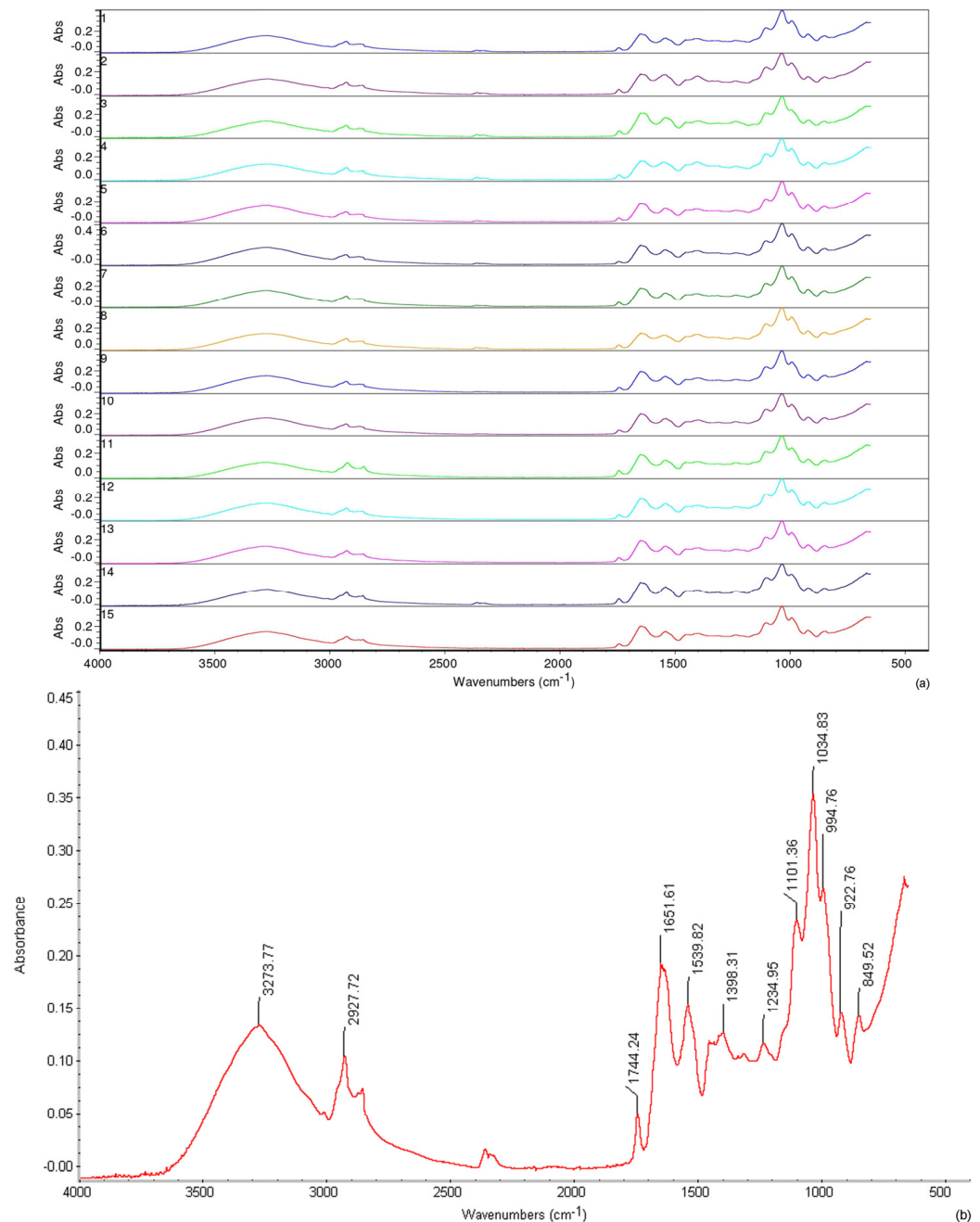

Figure 4. (**a**) FTIR spectra of *Camelina Sativa*-based biopolymer films (labels (runs) 1–15 refer to different processing conditions (see Table 1)). (**b**) Characteristic peaks for selected sample 14 with mean values of process parameters (experiment central point).

The peaks at 850, 920, 990, 1030, and 1100 cm^{-1} demonstrated the presence of glycerol in the film structure, as confirmed by analyses of a pure glycerol spectrum by Petraru and Amariei [49]. All the obtained peaks point to the composite CSoC film's structure: predominantly protein structure, but with a presence of polysaccharides, lipids, and cellulose. The presence of the plasticizer (glycerol) was also confirmed.

3.7. Antioxidative Activity—DPPH Assay

Table 1 displays the antioxidant properties of the studied CSoC-based films as assessed by the DPPH method. All tested films exhibited high antioxidant capacity at most applied process parameters (up to 78.04%), indicating that the developed films could be used as active films with significant antioxidant activity.

The significant antioxidant activity might be a consequence of the presence of phenolic compounds that cannot be removed because of their strong interaction with proteins. The antiradical activity estimated by DPPH, according to findings in the literature, is positively correlated with the total amount of polyphenols [74]. After the oil has been pressed from the seeds, almost all the phenolic compounds detected remain in the seed residues (cake) [75]. Synergism between polyphenols and water-soluble amino acids and their derivatives is favorable to high antioxidant activity, as it is known that peptides can act as antioxidants [76]. It was reported that six flavonoids (catechic acid, epicatechin, quercitrin, isoquercetin, rutin, and isorhamnetin), three hydroxybenzoic acids (proto-catechuic, p-hydroxybenzoic, and salicylic acids), and one hydroxycinnamic acid (sinapic) were identified in camelina oilseed cake [75,77].

The obtained results show that the radical scavenging activity of DPPH radicals was significantly lower (16.44%–29.13%) in the samples of CSoC-based films synthesized at pH 12. Lower pH values (pH 8) resulted in higher DPPH radical scavenging activity (70.55%–77.32%), independent of temperature and concentration variations. The antioxidant activity of some compounds in *Camelina sativa* is pH-dependent. Certain functional groups in highly alkaline conditions may degrade or lose their effectiveness. The pH changes that take place during film production and the subsequent drying process may have an effect on the chemical stability of these antioxidants.

3.8. Antimicrobial Activity—Disc Diffusion Method

In recent years, foodborne pathogenic bacteria such as *Escherichia coli*, *Salmonella typhimurium*, *Staphylococcus aureus*, and *Listeria monocytogenes* have represented a significant problem for the food industry, as it was shown that they can contaminate fresh products in different phases of product processing [78,79]. The presence of pathogens and spoilage microorganisms on the packaging surfaces has also been documented [80,81]. Therefore, this part of this study was carried out to assess the antibacterial activity of fifteen biopolymer films based on CSoC against two Gram-negative bacteria, *Escherichia coli* ATCC 10536 and *Salmonella typhimurium* ATCC 14028, and two Gram-positive bacteria, *Staphylococcus aureus* ATCC 25923 and *Listeria monocytogenes* ATCC 19111.

The antibacterial activity of the CSoC films was evaluated by measuring the diameter of the growth inhibition zones on the bacterial strains, and the results are presented in Table 2. The data showed that some films based on *Camelina sativa* oilseed cake clearly possess antibacterial properties against *S. aureus* ATCC 25923 (Figure 5), while some had a slight inhibitory effect on *S. typhimurium* ATCC 14028 (Table 2). These results are supported by the study of Răducu et al. [82], in which *Camelina sativa* extracts showed high antimicrobial activity against *S. typhimurium*, *Enterococcus faecalis*, and *S. aureus*. On the other hand, it was found that the tested CSoC-based films had no inhibitory effect on *E. coli* ATCC 10536 and *L. monocytogenes* ATCC 19111 and even had a stimulating effect on the *L. monocytogenes* growth (Figure 5). The enhancement effect observed in this study correlates with previous reports that some natural compounds promote the growth of microorganisms [83]. The specific investigation conducted by Sandasi et al. [84] also showed that some essential oil components promote the growth of *L. monocytogenes*. Overall, our results indicate a potential application of *Camelina sativa* for antimicrobial packaging material, as it has been shown that some samples have an inhibitory effect on bacterial growth, especially in *S. aureus*.

Table 2. Antimicrobial activity of CSoC-based films against bacteria *Escherichia coli* ATCC 10536, *Salmonella typhimurium* ATCC 14028, *Staphylococcus aureus* ATCC 25923, and *Listeria monocytogenes* ATCC 19111 (labels (runs) 1–15 refer to different processing conditions (see Table 1)).

	Zone of Inhibition (mm) against Bacteria			
	Gram-Negative Bacteria		**Gram-Positive Bacteria**	
Sample Number	*Escherichia coli* **ATCC 10536**	*Salmonella typhimurium* **ATCC 14028**	*Staphylococcus aureus* **ATCC 25923**	*Listeria monocytogenes* **ATCC 19111**
1.	-	-	10	-
2.	-	-	-	-
3.	-	-	12	-
4.	-	-	-	-
5.	-	-	10	-
6.	-	-	-	-
7.	-	-	8	-
8.	-	-	-	-
9.	-	-	-	-
10.	-	-	-	-
11.	-	-	9	-
12.	-	-	-	-
13.	-	9	10	-
14.	-	9	10	-
15.	-	8	9	-
Antibiotic:				
Ampicilin 10 mcg	9	9	15	10

"-" no antimicrobial activity. Values are expressed in zone of inhibition diameters (mm) and represent the mean value obtained in three independent replicates.
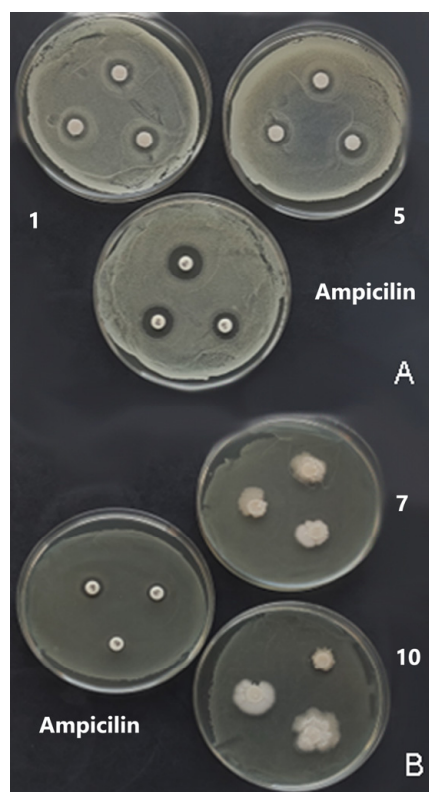

Figure 5. Antimicrobial activity of CSoC-based films against *Staphylococcus aureus* ATCC 25923 (**A**) and *Listeria monocytogenes* ATCC 19111 (**B**) (labels (runs) 1. 5, 7, and 10 refer to different processing conditions (see Table 1)).

3.9. Statistical Analysis

3.9.1. Principal Component Analysis

In PCA graphics, the closeness of points indicates shared patterns among them. The orientation of the variable vector in factor space illustrates the upward trend of those variables, and its length correlates proportionally with the squared correlation value between the fitted value and the variable. Additionally, the angles between variables indicate the degree of their correlations, with smaller angles signifying stronger correlations.

Figure 6 shows the PCA biplot diagram, which depicts the relationships between MC, S, thickness, TS, EB, WVP, and AO for CSoC-based film (runs 1–15) and demonstrates that the first two components accounted for a combined 36.92% and 26.16% of the total variance. In the first principal component (PC1), positive correlations were observed for S (22.7%), t (23.8%), and EB (14.8%), while negative correlations were noted for MC (23.0%), WVP (7.5%), and AO (8.3%) based on their coordinates. On the other hand, the second principal component (PC2) displayed positive associations with S (7.4%) and TS (29.2%), whereas t (8.1%), EB (14.8%), WVP (16.1%), and AO (20.6%) exhibited negative relationships with PC2.
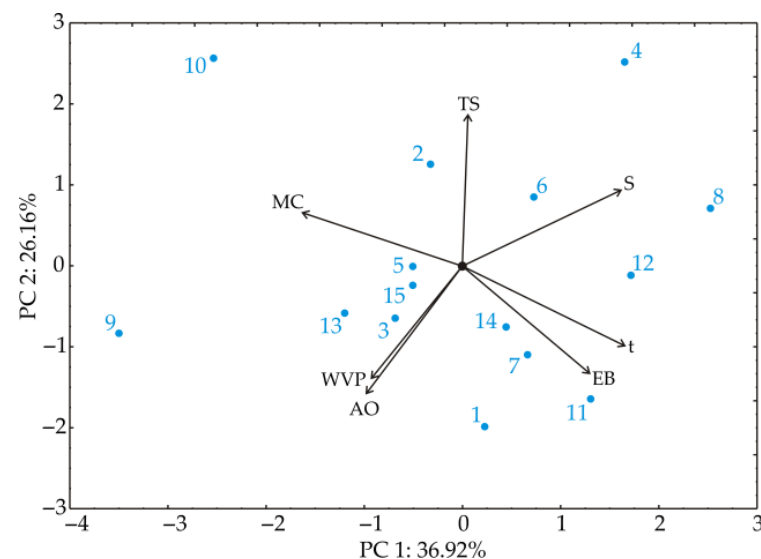

Figure 6. The PCA biplot diagram depicting the relationships among MC (moisture content), S (solubility), thickness, TS (tensile strength), EB (elongation at break), WVP (water vapor permeability), and AO (antioxidative potential) for CSoC-based film (runs 1–15).

3.9.2. Color Correlation Analysis

To illustrate the significance of the correlation coefficients between various responses, a color correlation diagram was created (Figure 7). Blue was used to represent positive correlations, and red was used to represent negative correlations. The strength of these relationships was represented by the size of the circles in the diagram [85]. The correlation analysis revealed statistically significant relationships ($p < 0.001$) between S and AO. Additionally, MC displayed a negative correlation with t (correlation coefficient r = -0.727, $p < 0.01$). Conversely, a positive correlation was found between t and EB (r = -0.538, $p < 0.05$), while TS exhibited a negative relationship with WVP (r = -0.535, $p < 0.05$).
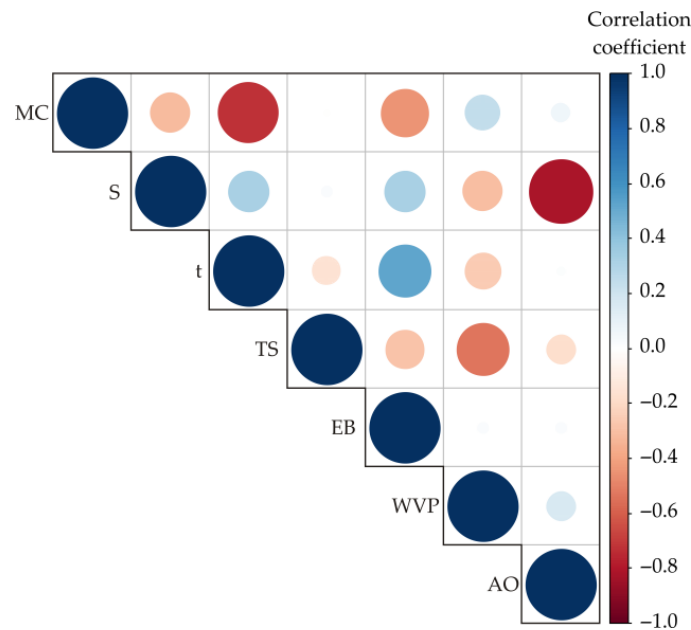
Figure 7. Color correlation diagram between the observed responses.

3.9.3. Standard Score Optimization

The optimal score was determined by averaging the scores for all product parameters (MC, S, t, TS, EB, WVP, and AO). Through the maximal score function, the ideal factor variables and the optimal levels for the film-making process were determined. These findings are shown in Figure 8. The optimal combination of all tested responses is shown by the total Z-score values, which mathematically summarize all segment Z-scores. Sample 12 yielded the highest score (0.687), showcasing optimized parameters at pH = 10, temperature = 100 °C, and concentration = 5. Under these specific conditions, the film-making process resulted in the following values: MC = 13.86%, S = 34.52%, t = 292.6 μm, TS = 1.03 MPa, EB = 8.83%, WVP = 5.86 g/m^{2}h, and AO = 66.01% (refer to Table 1). Sample 12 resulted in an optimal combination of the investigated physico-chemical, mechanical, barrier, and antioxidant properties and achieved an optimal combination of the observed quality characteristics among the tested film formulations (samples 1–15, Table 1).
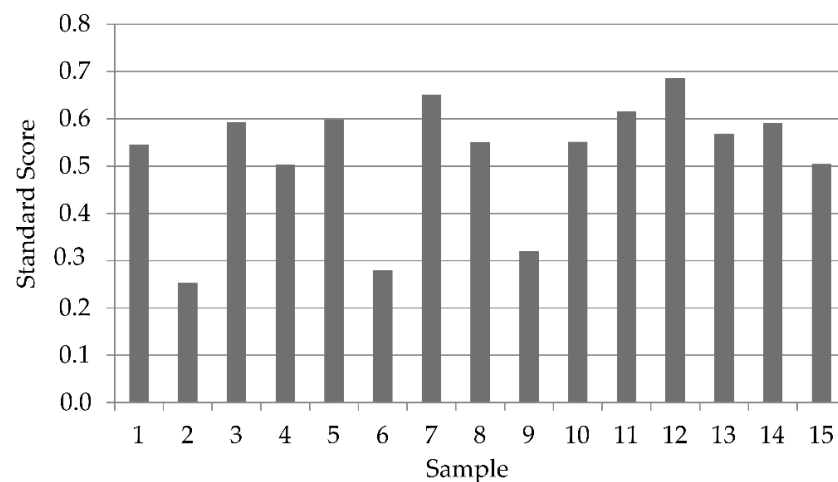

Figure 8. Z-score analysis of properties of the obtained CSoC-based films (labels (runs) 1–15 refer to different processing conditions (see Table 1)).

3.9.4. Modeling of the Predictive Artificial Neural Network

Artificial neural network (ANN) models have emerged as highly effective mathematical tools, particularly in handling complex parameter structures with intricate nonlinear connections and relationships [86]. Their adaptability, precise predictive accuracy, robust generalization capabilities, and resilience to noisy data render ANN implementation a promising approach for modeling complex systems [87]. Given that biological materials entail dynamic, multifaceted environments characterized by numerous nonlinear interactions, this study aimed to harness ANN to develop a predictive model for film properties encompassing physico-chemical, mechanical, barrier, structural, and antioxidative aspects subjected to various process parameters (pH: 8–10–12, temperature: 60 °C–80 °C–100 °C, and concentration: 3%–4%–5%).

Tables 3 and 4 present the fundamental characteristics and performance metrics, respectively, of the developed models. These artificial neural network regression models were structured to forecast film properties, specifically MC, S, t, TS, EB, WVP, and AO. They exhibited commendable performance, denoted by high r^2 values, during both the training and testing phases, ranging between 0.951 and 1.000 for the testing cycle and between 0.559 and 0.992 for the training cycle.

Upon analysis using the ANN models, the optimal neuron counts for the hidden layers were determined to fall between 3 and 10 for predicting MC, S, t, TS, EB, WVP, and AO (as detailed in Table 3). Notably, these models demonstrated consistently high r^2 values during the learning phase, individually presented in Table 3.

Table 3. The performance of the developed regression model.

Parameters	No. of Neurons in Hidden Layer	Performance		Error		Train. Algorithm (BFGS)	Hidden Activation	Output Activation
		Train.	Test	Train.	Train.			
MC	5	0.951	0.559	0.715	27.243	10	Tanh	Tanh
S	9	1.000	0.992	0.243	0.661	218	Tanh	Tanh
t	3	1.000	0.744	2.167	176.711	11	Exp.	Exp.
TS	10	0.999	0.924	0.000	0.005	51	Log.	Exp.
EB	6	0.971	0.898	0.581	0.851	32	Exp.	Exp.
WVP	4	0.997	0.982	0.029	0.089	37	Exp.	Log.
AO	3	0.999	0.686	30.478	78.930	5	Log.	Log.

Table 4 illustrates the correspondence between the calculations made by the ANN models and the experimental data. The ANN model consistently predicted parameters across a wide range of values that were closely aligned with the experimental data, as indicated by the high r^2 values. Additionally, the calculated sum of square (SOS) values from the developed ANN models closely mirrored those documented in the existing literature [88,89]. A minimal lack of fit was observed in the models, signifying the model's satisfactory prediction of initial parameters (high r^2 value) and the minor variations in predicted data accounting for experimental values [90].

Table 4. Statistical error test and residual analysis of the developed regression models.

Response	χ^2	RMSE	MBE	MPE	SSE	AARD	r^2
MC	16.691	3.947	−1.527	11.625	233.670	11.625	0.688
S	0.760	0.842	0.240	1.457	10.638	1.457	0.989
t	278.927	16.135	0.600	4.967	3.9×10^3	4.967	0.809
TS	0.008	0.089	0.000	9.639	0.118	9.639	0.952
EB	0.242	0.475	0.009	2.961	3.389	2.961	0.976
WVP	0.096	0.299	0.113	3.107	1.345	3.107	0.977
AO	141.448	11.490	−1.321	24.116	1980.275	24.116	0.727

χ^2—chi squared test; RMSE—root mean square error; MBE—mean bias error; MPE—mean percentage error; SSE—sum squared error; AARD—average absolute relative deviation; r^2—coefficient of determination.

4. Practical Applications of CSoC in Food Packaging: Possibilities, Limitations, and Further Perspectives

CSoC-based biopolymer films, produced as a by-product of *Camelina sativa* oil extraction, offer a promising substitute for commercial food packaging applications. This reduces reliance on fossil fuels and promotes sustainability in the food and agriculture sectors. Moreover, biodegradable CSoC-based biopolymer films provide a more environmentally friendly overall footprint.

For any packaging material to be used practically, the production process's scalability is an essential component. The availability of *Camelina sativa* as a crop with the potential for large-scale cultivation is advantageous for CSoC-based biopolymer films. The whole value chain is more economically viable when by-products are used in film production. The challenges of scaling up the production of biopolymer materials from oil cakes include standardizing processing techniques, assuring product quality at higher volumes, and sourcing raw materials consistently and dependably.

The cost-effectiveness must be compared to currently available packaging materials and is dependent on many factors, including market demand, processing efficiency, and raw material availability. Crop yields, oil extraction techniques, and local farming methods all affect the price of oil cakes as a raw material. The costs of labor, energy, machinery, and processing have an impact on total production costs. It is anticipated that cost competitiveness with conventional packaging materials will increase as technology advances and production increases. Furthermore, it is crucial to adhere to current packaging standards and regulations. For biopolymer materials to be widely accepted, they must either meet or surpass the performance standards established by regulatory agencies.

Camelina sativa oil cake-based biopolymer films can be compared with other packaging materials, such as biopolymers and conventional plastics. The mechanical properties of the CSoC films compared with commercial materials underscore the potential of CSoC films while still being consistent with other oilseed cake-based films. The films are well suited for coating applications where a continuous and flexible structure is necessary for packaging and possible consumption due to their moderate mechanical properties. The potential applicability of CSoC films in food packaging is suggested by their low WVP. Good water resistance is indicated by the relatively low film solubility values, which is a crucial quality for preserving the structural integrity of films in aqueous environments. The films are good options for packaging materials intended to stop photo-oxidation and safeguard light-sensitive food products because of their low visible light transmission and ability to block UV radiation below 400 nm. The moderate antimicrobial activity and high antioxidative capacity of CSoC films indicate their potential as active packaging materials. The films can be made to meet or exceed the requirements needed for a variety of food packaging applications by optimizing the processing conditions.

To improve the characteristics of biopolymer materials and increase their competitiveness against conventional materials, continuous research and development are necessary. Their eco-friendliness, scalability, biodegradability, and potential economic benefits render them a desirable choice for sectors looking for sustainable substitutes. Examining novel formulations and processing methods can help overcome the present limitations and increase the number of uses. Industry and scientific researchers working together can hasten the market's acceptance of biopolymer materials.

Even though this work is a major advancement in the use of *Camelina sativa* for biopolymer materials, more research is required to answer a few important issues. For practical applications in the food packaging industry, a deeper comprehension of the films' long-term stability and durability—particularly under varying storage conditions, light exposure, and temperature fluctuations—is essential. In order to address potential consumer acceptance and preference, a thorough assessment of the film's compatibility with various food types, regulatory compliance, and potential impacts on sensory attributes is necessary for the practical application of the optimal film found in this study. This study also demonstrated the potential of biopolymer films derived from camelina for active

packaging, but the precise mechanisms behind the antimicrobial and antioxidant activities need to be explained.

5. Conclusions

Camelina sativa is a promising oil crop and, as such, a raw material for many various applications, including bioproducts and biofuel production, food, feed, and pharmaceutical applications. The aim of this work is to extend the application range of Camelina to the field of biopolymer materials. Biopolymer films based on Camelina were synthesized under different synthesis conditions (by varying pH, temperature, and concentration).

The obtained CSoC films were opaque, dark in color, firm, and flexible with the smell of the camelina oilseed cake. Low TS (0.49–1.89 MPa) and EB values (4.34%–16.66%) point to application in the form of coatings. Naturally occurring lipid components in oil cake affected low WVP values; therefore, the samples with higher oil cake concentration were found to have lower WVP values. Low WVP values correspond to low water solubility values (20.58%–44.57%). Lower concentrations of camelina oil cake and medium pH contributed to the lower values of the water solubility.

Very low transmission in the UV region (less than 2%), which increases after 400 nm but does not exceed 6.2%, predetermines films based on CSoC to be used for packaging foods that are susceptible to oxidative changes catalyzed by UV light. FTIR analysis revealed the composite CSoC film's structure: basically protein but with a possible share of polysaccharides, lipids, and cellulose. An important aspect is the proven biological activity in terms of antimicrobial activity against *S. aureus* and inhibitory effect on *S. typhimurium*, as well as very high antioxidant activity. The radical scavenging activity of DPPH radicals was up to 78.04%, indicating the application of CSoC films in the field of active packaging.

Mathematical modeling of the obtained results pointed to the most important positive and negative correlations between the obtained parameters. The lowest values of MC, S, and WVP and the highest values of TS, EB, and AO were set as optimal output variable values, and standard score analysis pointed to the sample obtained with the process parameters pH = 10, temperature = 100 °C, and concentration = 5% as optimal. The next research step will focus on the application of the optimal film for food packaging.

Author Contributions: Conceptualization, D.Š., S.R. and N.S.; methodology, N.S., D.Š. and R.T.; software, L.P.; validation, L.P. and D.Š.; formal analysis, R.T., N.S. and D.Š.; investigation, N.S., D.Š. and R.T.; resources, S.R. and N.S.; data curation, L.P.; writing—original draft preparation, D.Š.; writing—review and editing, S.R. and N.H.; visualization, S.P.; supervision, D.Š., S.R. and N.H.; project administration, D.Š.; funding acquisition, S.P. All authors have read and agreed to the published version of the manuscript.

Data Availability Statement: Data are contained within the article.

Conflicts of Interest: The authors declare no conflicts of interest.

References

1. Jamwal, V.; Mittal, A.; Dhaundiyal, A. Valorization of agro-industrial waste in composite films for sustainable packaging applications. *Mater. Today Proc.* **2023**. [CrossRef]
2. Klai, N.; Yadav, B.; El Hachimi, O.; Pandey, A.; Sellamuthu, B.; Tyagi, R.D. Chapter 18-Agro-Industrial Waste Valorization for Biopolymer Production and Life-Cycle Assessment Toward Circular Bioeconomy. In *Biomass, Biofuels, Biochemical*; Pandey, A., Tyagi, R.D., Varjani, S., Eds.; Elsevier: Amsterdam, The Netherlands, 2021; pp. 515–555. [CrossRef]

3. Sharmila, G.; Muthukumaran, C.; Manoj Kumar, N.; Sivakumar, V.M.; Thirumarimurugan, M. Chapter 12—Food waste valorization for biopolymer production. In *Current Developments in Biotechnology and Bioengineering*; Varjani, S., Pandey, A., Gnansounou, E., Khanal, S.K., Raveendran, S., Eds.; Elsevier: Amsterdam, The Netherlands, 2020; pp. 233–249. [CrossRef]

4. Sani, I.K.; Masoudpour-Behabadi, M.; Sani, M.A.; Motalebinejad, H.; Juma, A.S.M.; Asdagh, A.; Eghbaljoo, H.; Khodaei, S.M.; Rhim, J.-W.; Mohammadi, F. Value-added utilization of fruit and vegetable processing by-products for the manufacture of biodegradable food packaging films. *Food Chem.* **2023**, *405 Pt B*, 134964. [CrossRef]

5. Galanakis, C.M. Sustainable Applications for the Valorization of Cereal Processing By-Products. *Foods* **2022**, *11*, 241. [CrossRef] [PubMed]

6. Šimat, V. Chapter 26—Valorization of seafood processing by-products. In *Valorization of Agri-Food Wastes and By-Products*; Bhat, R., Ed.; Academic Press: Cambridge, MA, USA, 2021; pp. 515–536. [CrossRef]

7. Lionetto, F.; Esposito Corcione, C. Recent Applications of Biopolymers Derived from Fish Industry Waste in Food Packaging. *Polymers* **2021**, *13*, 2337. [CrossRef] [PubMed]

8. Awasthi, M.K.; Paul, A.; Kumar, V.; Sar, T.; Kumar, D.; Sarsaiya, S.; Liu, H.; Zhang, Z.; Binod, P.; Sindhu, R.; et al. Recent trends and developments on integrated biochemical conversion process for valorization of dairy waste to value added bioproducts: A review. *Bioresour. Technol.* **2022**, *344*, 126193. [CrossRef]

9. Popović, S.; Hromiš, N.; Šuput, D.; Bulut, S.; Romanić, R.; Lazić, V. Chapter 3—Valorization of by-products from the production of pressed edible oils to produce biopolymer films. In *Cold Pressed Oils*; Ramadan, M.F., Ed.; Academic Press: Cambridge, MA, USA, 2020; pp. 15–30. [CrossRef]

10. Sharma, V.; Tsai, M.-L.; Nargotra, P.; Chen, C.-W.; Kuo, C.-H.; Sun, P.-P.; Dong, C.-D. Agro-Industrial FoodWaste as a Low-Cost Substrate for Sustainable Production of Industrial Enzymes: A Critical Review. *Catalysts* **2022**, *12*, 1373. [CrossRef]

11. USDA. Oilseeds: World Markets and Trade. United States Department of Agriculture Foreign Agricultural Service. 2023. Available online: https://www.fas.usda.gov/data/oilseeds-world-markets-and-trade (accessed on 20 November 2023).

12. Petraru, A.; Amariei, S.A. Novel Approach about Edible Packaging Materials Based on Oilcakes—A Review. *Polymers* **2023**, *15*, 3431. [CrossRef] [PubMed]

13. Mirpoor, S.F.; Giosafatto, C.V.L.; Mariniello, L.; D'Agostino, A.; D'Agostino, M.; Cammarota, M.; Schiraldi, C.; Porta, R. Argan (*Argania spinosa* L.) Seed Oil Cake as a Potential Source of Protein-Based Film Matrix for Pharmaco-Cosmetic Applications. *Int. J. Mol. Sci.* **2022**, *23*, 8478. [CrossRef]

14. Arshad, M.; Mohanty, K.A.; Acker, R.V.; Riddle, R.; Todd, J.; Khalil, H.; Misra, M. Valorization of Camelina Oil to Biobased Materials and Biofuels for New Industrial Uses A Review. *RSC Adv.* **2022**, *12*, 27230–27245. [CrossRef]

15. Neupane, D.; Lohaus, R.H.; Solomon, J.K.Q.; Cushman, J.C. Realizing the Potential of *Camelina sativa* as a Bioenergy Crop for a Changing Global Climate. *Plants* **2022**, *11*, 772. [CrossRef]

16. Mohammed, Y.A.; Chen, C.; Afshar, R.K. Nutrient requirements of Camelina for biodiesel feedstock in Central Montana. *Agron. J.* **2017**, *109*, 309–316. [CrossRef]

17. Bacenetti, J.; Restuccia, A.; Schillaci, G.; Failla, S. Biodiesel production from unconventional oilseed crops (*Linum usitatissimum* L. and *Camelina sativa* L.) in Mediterranean conditions: Environmental sustainability assessment. *Renew. Energy* **2017**, *112*, 444–456. [CrossRef]

18. Juodka, R.; Nainiene, R.; Juškiene, V.; Juška, R.; Leikus, R.; Kadžiene, G.; Stankeviciene, D. Camelina (*Camelina sativa* (L.) Crantz) as Feedstuffs in Meat Type Poultry Diet: A Source of Protein and n-3 Fatty Acids. *Animals* **2022**, *12*, 295. [CrossRef] [PubMed]

19. Lopez, C.; Sotin, H.; Rabesona, H.; Novales, B.; Le Quéré, J.-M.; Froissard, M.; Faure, J.-D.; Guyot, S.; Anton, M. Oil Bodies from Chia (*Salvia hispanica* L.) and Camelina (*Camelina sativa* L.) Seeds for Innovative Food Applications: Microstructure, Composition and Physical Stability. *Foods* **2023**, *12*, 211. [CrossRef] [PubMed]

20. Kurasiak-Popowska, D.; Stuper-Szablewska, K. The phytochemical quality of *Camelina sativa* seed and oil. *Acta Agric. Scand. B Soil Plant Sci.* **2020**, *70*, 39–47. [CrossRef]

21. Ilić, P.N.; Rakita, S.M.; Spasevski, N.J.; Đuragić, O.M.; Marjanović Jeromela, A.M.; Cvejić, S.; Zanetti, F. Nutritive value of serbian camelina genotypes as an alternative feed ingredient. *Food Feed Res.* **2022**, *49*, 209–221. [CrossRef]

22. Yang, Y.; Gupta, V.K.; Du, Y.; Aghbashlo, M.; Show, P.L.; Pan, J.; Tabatabaei, M.; Rajaei, A. Potential application of polysaccharide mucilages as a substitute for emulsifiers: A review. *Int. J. Biol. Macromol.* **2023**, *242*, 124800. [CrossRef]

23. Soukoulis, C.; Gaiani, C.; Hoffmann, L. Plant seed mucilage as emerging biopolymer in food industry applications. *Curr. Opin. Food Sci.* **2018**, *22*, 28–42. [CrossRef]

24. Ubeyitogullari, A.; Ciftci, O.N. Fabrication of bioaerogels from camelina seed mucilage for food applications. *Food Hydrocoll.* **2020**, *102*, 105597. [CrossRef]

25. Sydor, M.; Kurasiak-Popowska, D.; Stuper-Szablewska, K.; Rogozinski, T. Camelina sativa. Status quo and future perspectives. *Ind. Crops Prod.* **2022**, *187*, 115531. [CrossRef]

26. Mondor, M.; Hernández-Álvarez, A.J. *Camelina sativa* Composition, Attributes, and Applications: A Review. *Eur. J. Lipid Sci. Technol.* **2022**, *124*, 2100035. [CrossRef]

27. Šuput, D.Z.; Popović, S.Z.; Hromiš, N.M.; Rakita, S.M.; Spasevski, N.J.; Lončar, B.; Erceg, T.D.; Knežević, V.M. The influence of oil cake granulation and ultrasonic pretreatment on the properties of biopolymer films based on *Camelina sativa* oilseed cake. *Food Feed Res.* **2023**, *2023*, 61–75. [CrossRef]

28. Saberi, B.; Thakur, R.; Bhuyan, D.J.; Vuong, Q.V.; Chockchaisawasdee, S.; Golding, J.B.; Scarlett, C.J.; Stathopoulos, C.E. Development of edible blend films with good mechanical and barrier properties from pea starch and guar gum. *Starch. Stärke* **2017**, *69*, 1600227. [CrossRef]

29. *ISO 527-3:2018*; Plastics-Determination of Tensile Properties. Part 3: Test Conditions for Films and Sheets. International Organization for Standardization: Geneva, Switzerland, 2018.

30. *ISO 2528:2017*; Sheet Materials. Determination of Water Vapor Transmission Rate (WVTR). Gravimetric (Dish) Method. International Organization for Standardization: Geneva, Switzerland, 2017.

31. *ASTM D5576:00*; Standard Practice for Determination of Structural Features in Polyolefins and Polyolefin Copolymers by Infrared Spectrophotometry (FT-IR). ASTM International: West Conshohocken, PA, USA, 2021.

32. Razmavar, S.; Abdulla, M.A.; Ismail, S.B.; Hassandarvish, P. Antibacterial activity of leaf extracts of Baeckea frutescens against methicillin-resistant Staphylococcus aureus. *BioMed. Res. Int.* **2014**, *2014*, 5. [CrossRef] [PubMed]

33. Hajnal, E.J.; Babič, J.; Pezo, L.; Banjac, V.; Čolović, R.; Kos, J.; Krulj, J.; Pavšič-Vrtač, K.; Jakovac-Strajn, B. Effects of extrusion process on Fusarium and Alternaria mycotoxins in whole grain triticale flour. *LWT* **2022**, *155*, 112926. [CrossRef]

34. Nguyen, Q.H.; Ly, H.B.; Ho, L.S.; Al-Ansari, N.; Le, H.V.; Tran, V.Q.; Prakash, I.; Pham, B.T. Influence of data splitting on performance of machine learning models in prediction of shear strength of soil. *Math. Probl. Eng.* **2021**, *2021*, 1–15. [CrossRef]

35. Voća, N.; Pezo, L.; Jukić, Ž.; Lončar, B.; Šuput, D.; Krička, T. Estimation of the storage properties of rapeseeds using an artificial neural network. *Ind. Crops Prod.* **2022**, *187*, 115358. [CrossRef]

36. Brandić, I.; Pezo, L.; Bilandžija, N.; Peter, A.; Šurić, J.; Voća, N. Comparison of Different Machine Learning Models for Modelling the Higher Heating Value of Biomass. *Mathematics* **2023**, *11*, 2098. [CrossRef]

37. Rajković, D.; Jeromela, A.M.; Pezo, L.; Lončar, B.; Grahovac, N.; Špika, A.K. Artificial neural network and random forest regression models for modelling fatty acid and tocopherol content in oil of winter rapeseed. *J. Food Compos. Anal.* **2023**, *115*, 105020. [CrossRef]

38. Erdem, B.G.; Kaya, S. Characterization and application of novel composite films based on soy protein isolate and sunflower oil produced using freeze drying method. *Food Chem.* **2022**, *366*, 130709. [CrossRef]

39. Shen, Z.; Kamdem, D.P. Development and characterization of biodegradable chitosan films containing two essential oils. *Int. J. Biol. Macromol.* **2015**, *74*, 289–296. [CrossRef] [PubMed]

40. Sánchez-González, L.; Vargas, M.; González-Martínez, C.; Chiralt, A.; Cháfer, M. Characterization of edible films based on hydroxypropylmethylcellulose and tea tree essential oil. *Food Hydrocoll.* **2009**, *23*, 2102–2109. [CrossRef]

41. Benavides, S.; Villalobos-Carvajal, R.; Reyes, J.E. Physical, mechanical and antibacterial properties of alginate film: Effect of the crosslinking degree and oregano essential oil concentration. *J. Food Eng.* **2012**, *110*, 232–239. [CrossRef]

42. Salgado, P.R.; López-Caballero, M.E.; Gómez-Guillén, M.C.; Mauri, A.N.; Montero, M.P. Sunflower protein films incorporated with clove essential oil have potential application for the preservation of fish patties. *Food Hydrocoll.* **2013**, *33*, 74–84. [CrossRef]

43. Teixeira, B.; Marques, A.; Pires, C.; Ramos, C.; Batista, I.; Saraiva, J.A.; Nunes, M.L. Characterization of fish protein films incorporated with essential oils of clove, garlic and origanum: Physical, antioxidant and antibacterial properties. *LWT* **2014**, *59*, 533–539. [CrossRef]

44. Atarés, L.; De Jesús, J.; Talens, P.; Chiralt, A. Characterization of SPI-based edible films incorporated with cinnamon or ginger essential oils. *J. Food Eng.* **2010**, *99*, 384–391. [CrossRef]

45. Bulut, S. Research of Obtaining, Characterization and Optimization of Properties of Active, Biodegradable, Packaging Material Based on Pumpkin Oil Cake. Ph.D. Thesis, University of Novi Sad, Novi Sad, Serbia, 2021.

46. Šuput, D.; Lazić, V.; Popović, S.; Hromiš, N.; Bulut, S.; Pezo, L.; Banićević, J. Effect of process parameters on biopolymer films based on sunflower oil cake. *J. Process. Energy Agric.* **2018**, *22*, 125–128. [CrossRef]

47. Mirpoor, S.F.; Zannini, D.; Santagata, G.; Giosafatto, C.V.L. Cardoon seed oil cake proteins as substrate for microbial transglutaminase: Their application as matrix for bio-based packaging to extend the shelf-life of peanuts. *Food Hydrocoll.* **2024**, *147*, 109339. [CrossRef]

48. Jang, S.-A.; Lim, G.-O.; Song, K.B. Preparation and Mechanical Properties of Edible Rapeseed Protein Films. *J. Food Sci.* **2011**, *76*, C218–C223. [CrossRef]

49. Petraru, A.; Amariei, S. Sunflower Oilcake as a Potential Source for the Development of Edible Membranes. *Membranes* **2022**, *12*, 789. [CrossRef]

50. Popović, S. The Study of Production and Characterization of Biodegradable, Composite Films Based on Plant Proteins. Ph.D. Thesis, University of Novi Sad, Novi Sad, Serbia, 2013.

51. Bulut, S.; Popović, S.; Hromiš, N.; Šuput, D.; Adamović, D.; Lazić, V. Incorporation of essential oils into pumpkin oil cake-based materials in order to improve their properties and reduce water sensitivity. *Hem. Ind.* **2020**, *74*, 313–325. [CrossRef]

52. Abdollahi, M.; Damirchi, S.; Shafafi, M.; Rezaei, M.; Ariaii, P. Carboxymethyl cellulose-agar biocomposite film activated with summer savory essential oil as an antimicrobial agent. *Int. J. Biol. Macromol.* **2019**, *126*, 561–568. [CrossRef] [PubMed]

53. Hopkins, E.J.; Chang, C.; Lam, R.S.H.; Nickerson, M.T. Effects of flaxseed oil concentration on the performance of a soy protein isolate-based emulsion-type film. *Food Res. Int.* **2015**, *67*, 418–425. [CrossRef]

54. Pandiselvam, R.; Barut Gok, S.; Yüksel, A.N.; Tekgül, Y.; Çalıṣkan Koç, G.; Kothakota, A. Evaluation of the impact of UV radiation on rheological and textural properties of food. *J. Texture Stud.* **2022**, *53*, 800–808. [CrossRef] [PubMed]

55. Abdelhedi, O.; Nasri, R.; Jridi, M.; Kchaou, H.; Nasreddine, B.; Karbowiak, T. Composite bioactive films based on smooth-hound viscera proteins and gelatin: Physicochemical characterization and antioxidant properties. *Food Hydrocoll.* **2018**, *74*, 176–186. [CrossRef]

56. Fang, J.M.; Fowler, P.A.; Tomkinson, J.; Hill, C.A.S. The preparation and characterization of a series of chemically modified potato starches. *Carbohydr. Polym.* **2002**, *47*, 245–252. [CrossRef]

57. Priyadarshi, R.; Riahi, Z.; Rhim, J.-W. Antioxidant pectin/pullulan edible coating incorporated with Vitis vinifera grape seed extract for extending the shelf life of peanuts. *Postharvest Biol. Technol.* **2022**, *183*, 111740. [CrossRef]

58. Salgado, P.R.; López-Caballero, M.E.; Gómez-Guillén, M.C.; Mauri, A.N.; Montero, M.P. Exploration of the antioxidant and antimicrobial capacity of two sunflower protein concentrate films with naturally present phenolic compounds. *Food Hydrocoll.* **2012**, *29*, 374–381. [CrossRef]

59. Hager, A.-S.; Vallons, K.J.R.; Arendt, E.K. Influence of gallic acid and tannic acid on the mechanical and barrier properties of wheat gluten films. *J. Agric. Food Chem.* **2012**, *60*, 6157–6163. [CrossRef]

60. Chambi, H.N.M.; Lacerda, R.S.; Makishi, G.L.A.; Bittante, A.M.Q.B.; Gomide, C.A.; Sobral, P.J.A. Protein extracted from castor bean (*Ricinus communis* L.) cake in high pH results in films with improved physical properties. *Ind. Crops Prod.* **2014**, *61*, 217–224. [CrossRef]

61. Luo, Y.; Liu, H.; Yang, S.; Zeng, J.; Wu, Z. Sodium alginate-based green packaging films functionalized by guava leaf extracts and their bioactivities. *Materials* **2019**, *12*, 2923. [CrossRef]

62. Delgado, M.; Felix, M.; Bengoechea, C. Development of bioplastic materials: From rapeseed oil industry by products to added-value biodegradable biocomposite materials. *Ind. Crops Prod.* **2018**, *125*, 401–407. [CrossRef]

63. Jiang, L.; Zheng, K. Xanthoceras sorbifolium Bunge leaf extract activated chia seeds mucilage/chitosan composite film: Structure, performance, bioactivity, and molecular dynamics perspectives. *Food Hydrocoll.* **2023**, *144*, 109050. [CrossRef]

64. Rai, S.; Poonia, A. Formulation and characterization of edible films from pea starch and casein. *J. Pharmacogn. Phytochem.* **2019**, *8*, 317–321.

65. Šuput, D. Synthesis, Characterization, Optimization of Properties and Application of Edible Active Packaging Material Based on Starch. Ph.D. Thesis, University of Novi Sad, Novi Sad, Serbia, 2016.

66. Ağçeli, G.K. A new approach to nanocomposite carbohydrate polymer films: Levan and chia seed mucilage. *Int. J. Biol. Macromol.* **2022**, *218*, 751–759. [CrossRef] [PubMed]

67. Lun, L.W.; Anas, A.; Gunny, N.; Kasim, F.H. Fourier Transform Infrared Spectroscopy (FTIR) analysis of Paddy Straw Pulp treated using Deep Eutectic Solvent. *AIP Conf. Proc.* **2017**, *1835*, 20049. [CrossRef]

68. Chen, Y.; Duan, Q.; Yu, L.; Xie, F. Thermomechanically processed chitosan:gelatin films being transparent, mechanically robust and less hygroscopic. *Carbohydr. Polym.* **2021**, *272*, 118522. [CrossRef] [PubMed]

69. Riyanta, A.B.; Riyanto, S.; Lukitaningsih, E.; Rohman, A. The employment of Fourier Transform Infrared Spectroscopy (FTIR) and chemometrics for analysis of candlenut oil in binary mixture with grape seed oil. *Food Res.* **2020**, *4*, 184–190. [CrossRef] [PubMed]

70. Wachirattanapongmetee, K.; Katekaew, S.; Weerapreeyakul, N.; Thawornchinsombut, S. Differentiation of protein types extracted from tilapia byproducts by FTIR spectroscopy combined with chemometric analysis and their antioxidant protein hydrolysates. *Food Chem.* **2024**, *437*, 137862. [CrossRef]

71. Ji, Y.; Yang, X.; Ji, Z.; Zhu, L.; Ma, N.; Chen, D.; Jia, X.; Tang, J.; Cao, Y. DFT-calculated IR spectrum amide I, II, and III band contributions of N-Methylacetamide fine components. *ACS Omega* **2020**, *5*, 8572–8578. [CrossRef]

72. Pradini, D.; Juwono, H.; Madurani, K.A.; Kurniawan, F. A preliminary study of identification halal gelatin using quartz crystal microbalance (QCM) sensor. *Mal. J. Fund. Appl. Sci.* **2018**, *14*, 325–330. [CrossRef]

73. Pan, P.; Kai, W.; Zhu, B.; Dong, T.; Inoue, Y. Polymorphous Crystallization and Multiple Melting Behavior of Poly(l-lactide): Molecular Weight Dependence. *Macromolecules* **2007**, *40*, 6898–6905. [CrossRef]

74. Mieriņa, I.; Adere, L.; Krasauska, K.; Zoltnere, E.; Skrastiņa, D.Z.; Jure, M. Antioxidant Properties of Oil and Press-Cakes. *Proc. Latv. Acad. Sci. B Nat. Exact Appl. Sci.* **2017**, *6*, 515–521. [CrossRef]

75. Terpinc, P.; Polak, T.; Makuc, D.; Poklar Ulrih, N.; Abramovič, H. The occurrence and characterisation of phenolic compounds in *Camelina sativa* seed, cake and oil. *Food Chem.* **2012**, *131*, 580–589. [CrossRef]

76. Jin, D.; Liu, X.; Zheng, X.; Wang, X.; He, J. Preparation of antioxidative corn protein hydrolysates, purification and evaluation of three novel corn antioxidant peptides. *Food Chem.* **2016**, *204*, 427–436. [CrossRef] [PubMed]

77. Li, F.; Li, Z.; Wei, Y.; Zhang, L.; Ning, E.; Yu, L.; Zhu, J.; Wang, X.; Ma, Y.; Fan, Y. Qualitative and quantitative analysis of polyphenols in camelina seed and their antioxidant activities. *Nat. Prod. Res.* **2023**, *37*, 1888–1891. [CrossRef] [PubMed]

78. Galié, S.; García-Gutiérrez, C.; Miguélez, E.M.; Villar, C.J.; Lombó, F. Biofilms in the food industry: Health aspects and control methods. *Front. Microbiol.* **2018**, *9*, 898. [CrossRef]

79. Tomičić, Z.; Čabarkapa, I.; Čolović, R.; Đuragić, O.; Tomičić, R. Salmonella in the feed industry: Problems and potential solutions. *J. Agron. Technol. Eng. Manag.* **2019**, *2*, 130–137.

80. Siroli, L.; Patrignani, F.; Serrazanetti, D.I.; Chiavari, C.; Benevelli, M.; Grazia, L.; Lanciotti, R. Survival of spoilage and pathogenic microorganisms on cardboard and plastic packaging materials. *Front. Microbiol.* **2017**, *8*, 2606. [CrossRef]

81. Tomičić, R.; Tomičić, Z.; Thaler, N.; Humar, M.; Raspor, P. Factors influencing adhesion of bacteria Escherichia coli, Pseudomonas aeruginosa, Staphylococcus aureus and yeast Pichia membranifaciens to wooden surfaces. *Wood Sci. Technol.* **2020**, *54*, 1663–1676. [CrossRef]

82. Răducu, A.L.; Popa, A.; Sicuia, O.; Boiu-Sicuia, O.A.; Israel-Roming, F.; Cornea, C.P.; Jurcoane, S. Antimicrobial activity of camelina oil and hydroalcoholic seed extracts. *Rom. Biotecnol. Lett.* **2021**, *26*, 2355–2360. [CrossRef]

83. Ofek, I.; Hasty, D.L.; Sharon, N. Anti-adhesion therapy of bacterial diseases: Prospects and problems. *FEMS Immunol. Med. Microbiol.* **2003**, *38*, 181–191. [CrossRef] [PubMed]

84. Sandasi, M.; Leonard, C.M.; Viljoen, A.M. The effect of five common essential oil components on Listeria monocytogenes biofilms. *Food Control* **2008**, *19*, 1070–1075. [CrossRef]

85. Ćurčić, L.; Lončar, B.; Pezo, L.; Stojić, N.; Prokić, D.; Filipović, V.; Pucarević, M. Chemometric Approach to Pesticide Residue Analysis in Surface Water. *Water* **2022**, *14*, 4089. [CrossRef]

86. Ring, M.; Wunderlich, S.; Scheuring, D.; Landes, D.; Hotho, A. A survey of network-based intrusion detection data sets. *Comput. Secur.* **2019**, *86*, 147–167. [CrossRef]

87. Sharma, R.; Kamble, S.S.; Gunasekaran, A.; Kumar, V.; Kumar, A. A systematic literature review on machine learning applications for sustainable agriculture supply chain performance. *Comput. Oper. Res.* **2020**, *119*, 104926. [CrossRef]

88. Kollo, T.; von Rosen, D. Chapter 4—Multivariate Linear Models. In *Advanced Multivariate Statistics with Matrices*; Hazewinkel, M., Ed.; Springer: Dordrecht, The Netherlands, 2005; pp. 355–472. [CrossRef]

89. Doumpos, M.; Zopounidis, C. Preference disaggregation and statistical learning for multicriteria decision support: A review. *Eur. J. Oper. Res.* **2011**, *209*, 203–214. [CrossRef]

90. Turányi, T.; Tomlin, A.S. *Analysis of Kinetic Reaction Mechanisms*; Springer: Berlin/Heidelberg, Germany, 2014; Volume 20, pp. 5–359.